

A Novel DC Capacitor Voltage Balance Control Method for Cascade Multilevel STATCOM

Zhao Liu, Bangyin Liu, *Member, IEEE*, Shanxu Duan, and Yong Kang

Abstract—This paper presents a novel dc capacitor voltage balance control method for cascade multilevel static synchronous compensator (STATCOM) and a general analytical method for balance control strategy. Considering that the imbalance of dc capacitor voltage is caused by the inconsistency of active power absorbed and consumed by chain, a balance control strategy based on active voltage vector superposition is proposed, in which an active voltage component is superposed to chain's output voltage to change its absorbed active power. A general analytical method based on vector analysis is also presented, by which the performance of balance control strategy can be analyzed, including stability and regulation capacity. To find out the most appropriate balance control strategy, a comparison still based on vector analysis among the proposed and other two commonly used methods is provided, from which it can be known that the proposed balance control strategy has the advantage of good stability and strong regulation capacity, and simulations are performed to prove it. The effectiveness of proposed control scheme has been verified by experimental results based on a three-phase 36-chain cascade multilevel STATCOM laboratory prototype.

Index Terms—Cascade multilevel, dc capacitor voltage balance, static synchronous compensator (STATCOM), vector analysis.

I. INTRODUCTION

COMPARED with the conventional 12-pulse voltage-sourced converter static synchronous compensator (STATCOM), the cascade multilevel STATCOM has the following advantages: transformerless, small volume, high efficiency, individual phase control ability, redundancy, etc. [1]–[3], it has been widely studied recently.

As the dc capacitors of cascade multilevel STATCOM are all independent and the shunt loss, switching loss, and switching delay of each chain are different, the dc capacitors voltage will be unbalanced [4]. The unbalanced dc-link capacitor voltage will introduce some problems, such as the increase of the output voltage total harmonic distortion (THD). When the degree of unbalance increases, the capacitor voltage of some chains becomes higher than others, which affects the safety of the devices or leads to serious system collapse [5].

Manuscript received February 23, 2010; revised April 30, 2010; accepted May 2, 2010. Date of current version December 16, 2011. This work was supported in part by the National Natural Science Foundation of China under Project 50907027, in part by China Postdoctoral Science Foundation under Project 20080440932, and in part by the National Basic Research Program (973 Program) of China under Project 2009CB219700. Recommended for publication by Associate Editor J. HR Enslin.

The authors are with the College of Electrical and Electronic Engineering, Huazhong University of Science and Technology, Wuhan 430074, China (e-mail: hustceee@gmail.com; lby@mail.hust.edu.cn; dshanxu@263.net; ykang@mail.hust.edu.cn).

Digital Object Identifier 10.1109/TPEL.2010.2050337

Previously, the selective harmonic elimination (SHE) was usually selected as modulation strategy for cascade multilevel STATCOM [6]–[8]. A balance control strategy based on swapping pulses is proposed in literature [6], in which all dc capacitors will be equally charged and balanced. This method is simple and does not need to detect all dc voltages, it can only eliminate the imbalances caused by the inconsistent drive pulse, but not those caused by other reasons, such as the difference of dc capacitors, switches, etc. Therefore, it is more inclined to achieve balance through closed-loop control now.

The balance control method based on ac bus energy exchange was proposed in [9]–[12], in which the dc voltages are coupled to a common ac bus through inverters to distribute active power among chains dynamically. Similarly, the method based on dc bus energy exchange was proposed in [13]. But both of the methods need additional hardware circuits and control systems, which will increase the system cost and complexity.

In recent years, the modulation strategy of carrier phase shift is usually adopted for cascade multilevel STATCOM [14]–[21], because this strategy is easier to achieve dc capacitor voltage balance by the way of closed-loop control compared with SHE. Regulation of phase-shift angle is the most commonly used balance control strategy [15]–[17], which changes the absorbed active power of each chain through changing the phase angle of its output voltage; this method is direct, however, the phase-shift angle is relatively small for large-capacity STATCOM and the inappropriate change of the phase-shift angle will cause the system unstable. An individual voltage balancing strategy (IVBS) has been proposed in [18] and [19] to realize independent modulation control of each chain, in which an active component is superposed to chain output voltage. However, the cosine value of the current phase angle is included in the denominator; therefore, the system becomes very sensitive to disturbance due to the zero-crossing point of the sine value. Another balance control method named individual balancing control is proposed in [20]–[22], in which a cosine component of system voltage is superposed to chain output voltage. But the disadvantage is with poor regulation capability under small reactive current and is easy to be affected by the accuracy of phase-locked loop (PLL).

Regulation capacity and stability are the most important evaluation index of balance control strategy. Any kind of balance control strategy has its own regulation range, and it could not achieve dc capacitor voltage balance control at full range; therefore, it is necessary to derive its maximum regulation range quantitatively, which can play a guiding role of system design and components selection; stability is related to the difficulty

of system control parameter design and a good control method should have strong robustness; therefore, it is essential to study the stability of balance control strategy deeply.

Many dc capacitor voltage balance control strategies have been proposed for cascade multilevel STATCOM in the present literatures, but the comparison among various balance control strategies has been rarely discussed, it is necessary to make a comparison among various methods in order to find out the most suitable one.

In this paper, a novel dc capacitor voltage balance control strategy based on active voltage vector superposition for cascade multilevel STATCOM is proposed, in which the actual phase current is used to regulate the absorbed active power of each chain to achieve balance control, and it can overcome the problems mentioned earlier in [18]–[22]. Furthermore, the way of vector analysis is presented; through this method, the stability and regulation capability of proposed control strategy is analyzed, and the maximum regulation range is quantitatively given. In order to find out the most appropriate balance control strategy, a comparison still based on vector analysis among three types of balance control strategy is presented, including comparison of stability and regulation capability.

This paper focuses on the dc capacitor voltage balance control for cascade multilevel STATCOM, which adopts carrier phase-shifting modulation strategy. The rest of paper is organized as follows. In Section II, three types of balance control strategy for cascade multilevel STATCOM through vector analysis of a single chain are concluded, and the balance control strategy based on active voltage vector superposition is proposed. Section III is devoted to present a new analytical way based on vector analysis for the proposed control strategy, including stability and regulation capability analysis. Section IV focuses on comparison among three types of balance control strategy, and the conclusion is verified by simulation. Section V will be devoted to validate the proposed control scheme through experimental results, followed by conclusions in Section VI.

II. BALANCE CONTROL STRATEGY BASED ON ACTIVE VOLTAGE VECTOR SUPERPOSITION

A. Vector Analysis of Cascade Multilevel STATCOM

The system diagram of delta-connected cascade multilevel STATCOM is shown in Fig. 1. In Fig. 1, u_{sa} , u_{sb} , and u_{sc} are the phase voltage of point of common coupling (PCC); u_{sab} , u_{sbc} , and u_{sca} are the line-to-line voltage of PCC; u_{rab} , u_{rbc} , and u_{rca} are the line-to-line voltage of STATCOM; i_{sab} , i_{sbc} , and i_{sca} are the phase current; the positive current direction is represented in the schema; u_{c1} , u_{c2} , \dots , u_{cN} are dc capacitor voltage of arbitrary link; L is the joint inductance; and N is the chain number.

Ignoring the series loss of cascade multilevel STATCOM, the system has three operation modes: capacitive mode, inductive model, and the no-load mode, the vector diagrams are shown in Fig. 2, respectively, where \dot{u}_s is the system voltage, \dot{u}_r is the

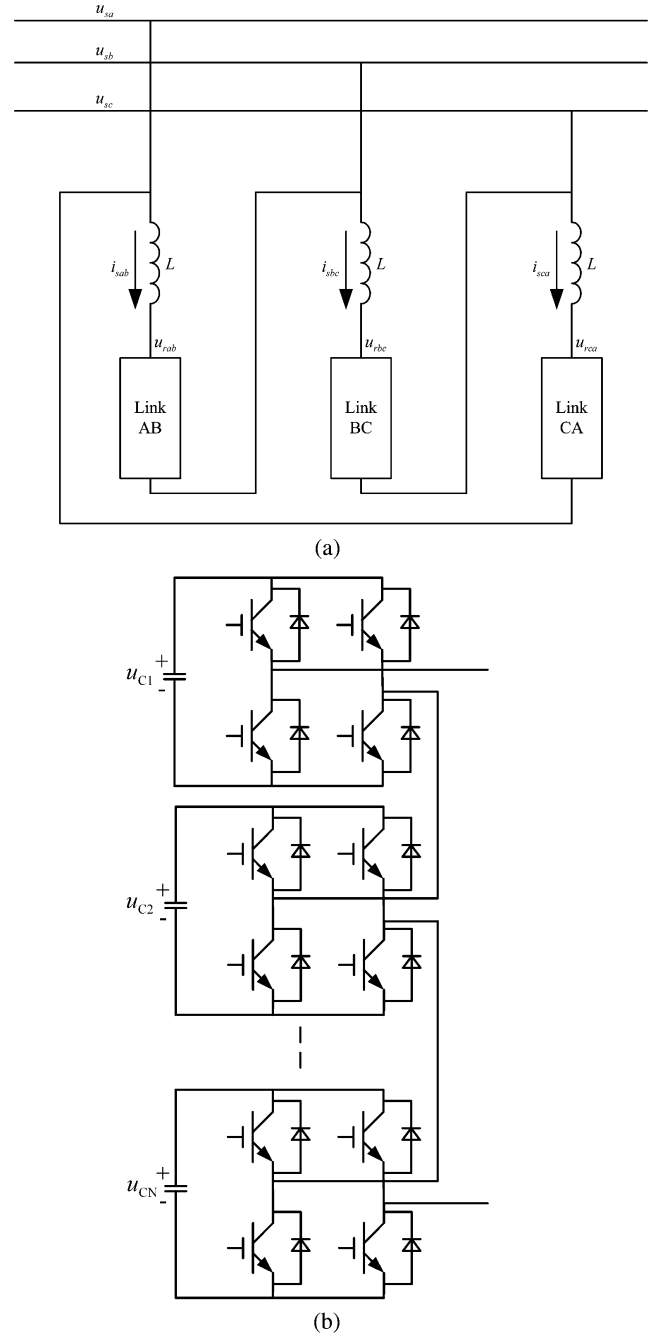


Fig. 1. System diagram of cascade multilevel STATCOM. (a) System connection diagram. (b) Circuit of single-phase link.

STATCOM output voltage, \dot{i}_s is the phase current, and \dot{u}_L is the voltage of joint inductance.

For simplicity, all the analyses are based on inductive mode, since the other two modes have the similar analysis methods and conclusions. When an arbitrary link is considered as study object, it can be equivalent into two series inverters through vector analysis of one chain and the remaining $N - 1$ chains of this link. When the dc capacitor voltage are balanced, and all chains are assumed to be the same and their dc-side voltage are u_{dc}^* and $(N - 1)u_{dc}^*$, respectively, there exist three vector operation modes with different modulation index, which is shown in

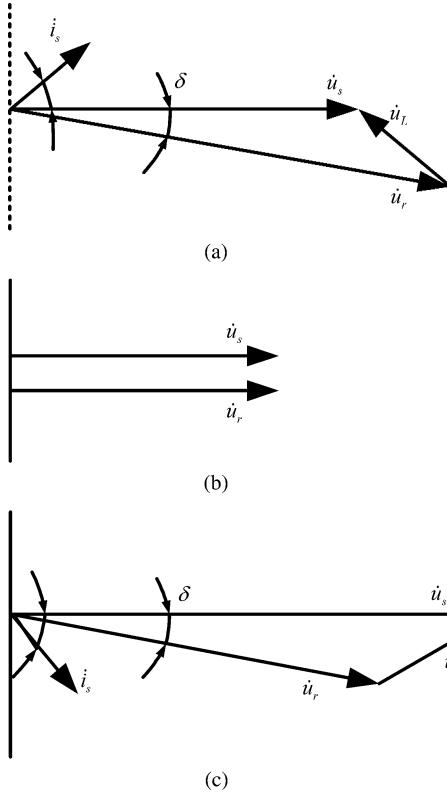


Fig. 2. Vector diagram of cascade multilevel STATCOM. (a) Capacitive mode. (b) No-load mode. (c) Inductive model.

Fig. 3, where the two circles represent the output voltage range of the inverters and P is the steady-state operating point, which is expressed as follows:

$$\begin{cases} u_{r1} = M(N-1)u_{dc}^* \\ u_{r2} = Mu_{dc}^* \\ u_r = u_{r1} + u_{r2} = MNu_{dc}^* \end{cases} \quad (1)$$

where M represents the modulation index and u_{dc}^* is the rated dc voltage of a single chain.

Generally, it is impossible to work at point P for the system because of differences among chains, which will produce an offset. For instance, the steady-state operating point in Fig. 3(a) can only be located in the shadow area, which is shown in Fig. 4(a) according to geometric analysis. The shadow area is the overlapping part of two circles, which means that the output u_r can only be synthesized in this area. In addition, the dc capacitor voltage of cascade multilevel STATCOM can only be maintained by absorbing active power from system; therefore, the absorbed active power of arbitrary chain is positive, and Fig. 4(b) shows the stable operation area of cascade multilevel STATCOM.

B. Balance Control Strategy Based on Active Vector Superposition

Fig. 5 illustrates circuit of an arbitrary chain and its vector diagram, where u_{rj} is the chain output voltage, θ_j is the angle

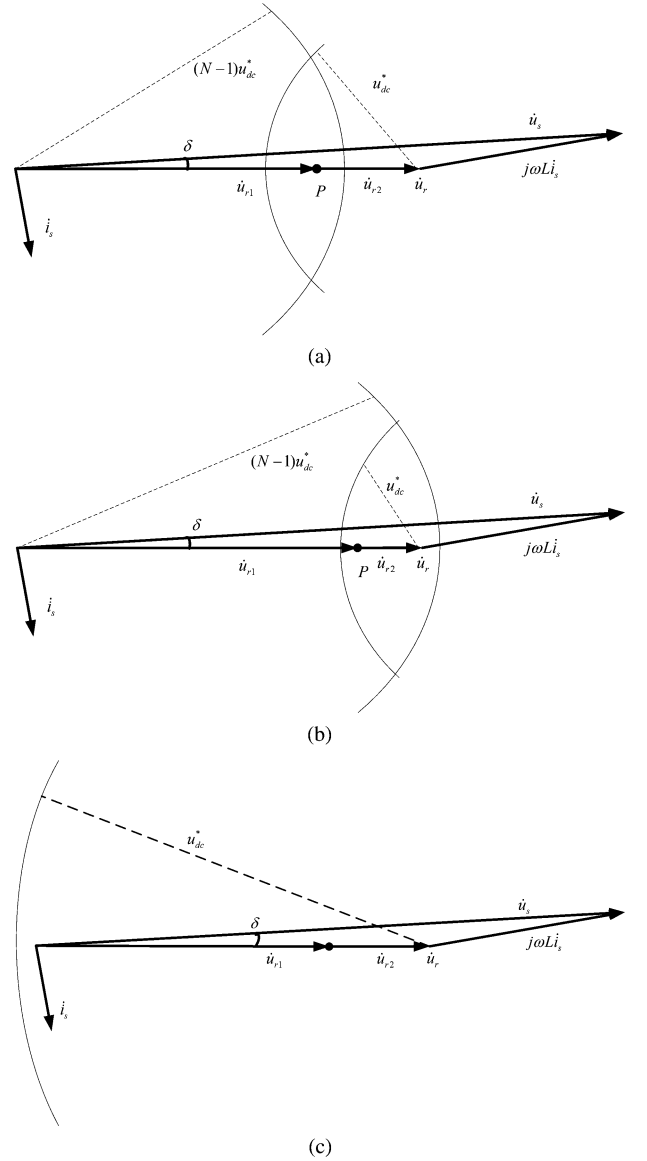


Fig. 3. Operation vector diagram with different modulation index. (a) Operation vector diagram when $(N-1)/N \leq M \leq 1$. (b) Operation vector diagram when $1/N \leq M \leq (N-1)/N$. (c) Operation vector diagram when $0 \leq M \leq 1/N$.

between them, u_{cj} is the dc-side voltage, and R_j is the equivalent shunt resistance, $j = 1, 2, \dots, N$.

According to active power balance, the variation of energy stored in capacitor depends on the absorbed active power and the consumption of the chain

$$P_{Cj} = P_{\text{absorb}} - P_{\text{loss}} = \frac{d(1/2Cu_{cj}^2)}{dt} \quad (2)$$

where P_{absorb} is the absorbed active power of the chain, U_{rj} is the rms value of output voltage, I_s is the rms value of phase current, and P_{loss} is the power loss of the chain, including dc-side power loss, switching loss, etc.

$$P_{\text{absorb}} = U_{rj} I_s \cos \theta_j. \quad (3)$$

According to (2), there are two ways to vary the dc-side voltage of chain, including regulation of the absorbed active power

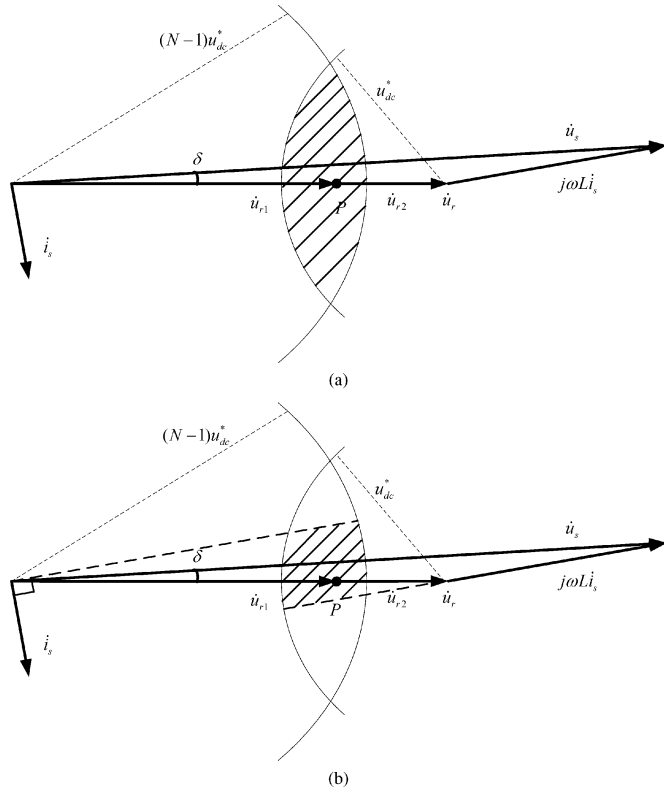


Fig. 4. Operation area of cascade multilevel STATCOM when $(N-1)/N \leq M \leq 1$. (a) Effective range of the output voltage vector. (b) Stable operation area.

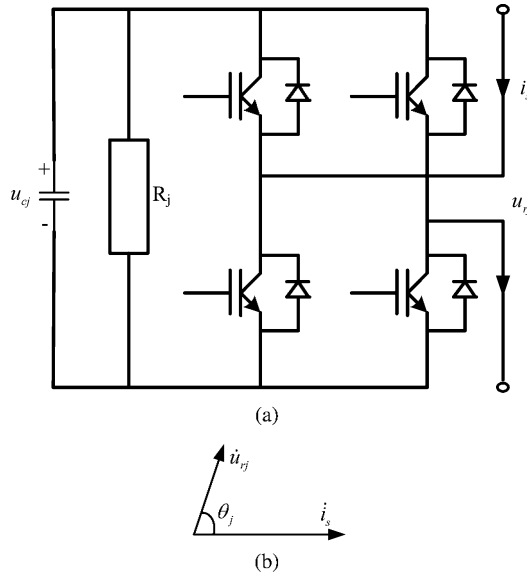


Fig. 5. Circuit and vector diagram of single chain. (a) Single chain circuit. (b) Single chain vector diagram.

and regulation of the consumed active power. As the power loss is fixed under fixed compensation current, the dc capacitor voltage balance can only be realized through regulation of the absorbed active power.

Equation (3) shows that there are three ways to change the absorbed active power of chain, including regulation of the output voltage magnitude, regulation of the phase current magnitude,

and regulation of the angle between them. As the magnitude and direction of current are fixed, only the magnitude and direction of chain output voltage can be changed, which corresponds to the chain controller output modulation index and phase-shift angle.

The dc capacitor voltage balance control for cascade multilevel STATCOM usually adopts hierarchical control structure, in which the total active and reactive power control is achieved by upper layer control; on this basis, the active power distribution among chains of homophase is achieved by lower layer control to realize dc voltage balance. Taking decouple control, for example, [23]–[25], the control diagram is shown in Fig. 6.

Therefore, according to the preceding analysis, the control strategy can be summarized as the following three steps:

- 1) modulation index regulation and maintain phase-shift angle;
- 2) phase-shift angle regulation and maintain modulation index;
- 3) regulation of both at the same time.

At present, most balance control strategies are based on the three methods mentioned earlier, a balance control strategy based on active voltage vector superposition is proposed on the basis of the third method, the control diagram is shown in Fig. 7, where K_p is the proportional coefficient.

The proposed control strategy is based on closed-loop control. Its basic idea is that a vector paralleled with phase current is superimposed to the output of upper layer control, which denotes a pure active voltage vector. All dc voltages must be detected, the reference voltage is the average value of homophase chains and the feedback is the actual value of each chain. If the feedback voltage is lower than the reference, a vector with the same direction of phase current is superimposed; *vice versa*, a vector with the opposite direction is superimposed, then the absorbed active power of each chain can be adjusted, while the balance control can be achieved.

III. VECTOR ANALYSIS OF BALANCE CONTROL STRATEGY BASED ON ACTIVE VOLTAGE SUPERPOSITION

Vector analysis includes two aspects: one is the stability of balance controller, it is supposed that the lower layer controller will not affect the upper layer controller for hierarchical control structure, otherwise, it will easily lead to instability of control systems; the other aspect is the regulatory capacity of balance control strategy, since the differences among chains are random and the power loss difference may be comparatively large, a good balance control strategy should have a strong regulatory capacity.

A. Stability Analysis of Balance Control Strategy

The vector diagram of proposed balance control strategy based on active voltage superposition is shown in Fig. 8. In Fig. 8, \dot{u}_{r2} becomes \dot{u}_{fs} after adding active voltage vector $\Delta\dot{u}_{fs}$, the active power absorbed of chain can be adjusted through changing the magnitude of $\Delta\dot{u}_{fs}$, then the dc voltage can be also maintained; at the same time, \dot{u}_{r1} becomes \dot{u}_{fc} after adding active voltage vector $-\Delta\dot{u}_{fs}$. The single-link vector diagram of

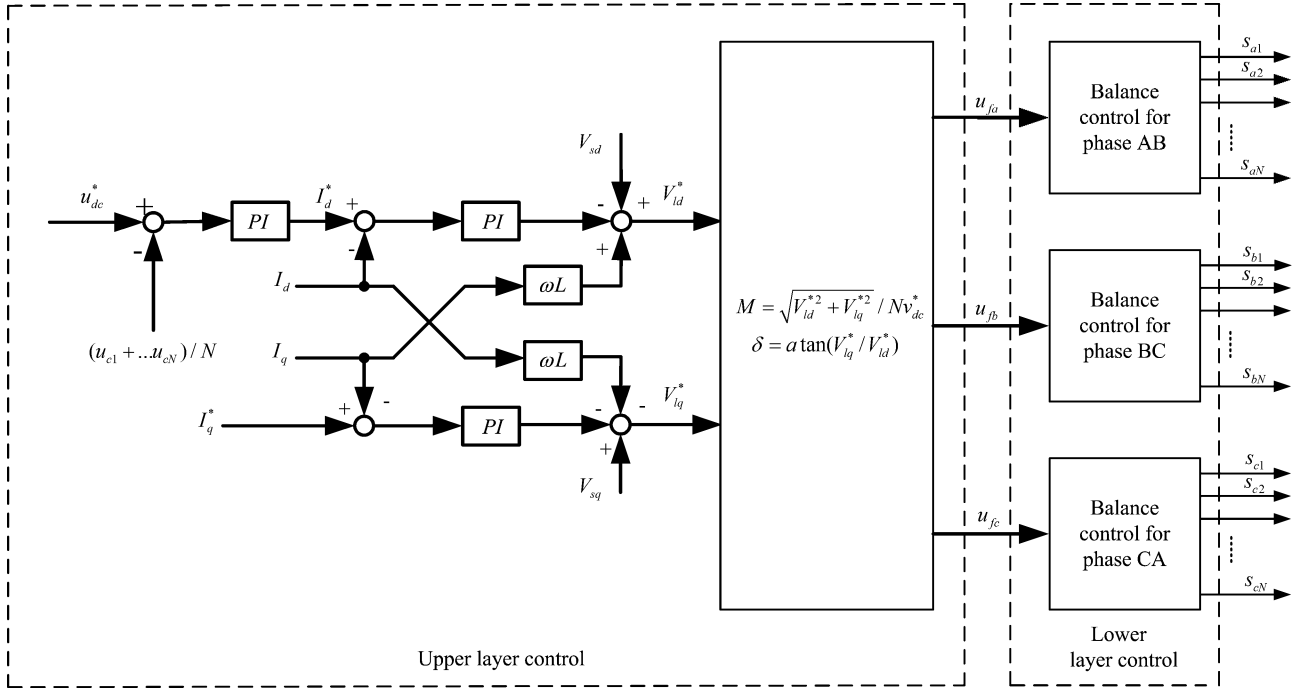


Fig. 6. Hierarchical controller for cascade multilevel STATCOM.

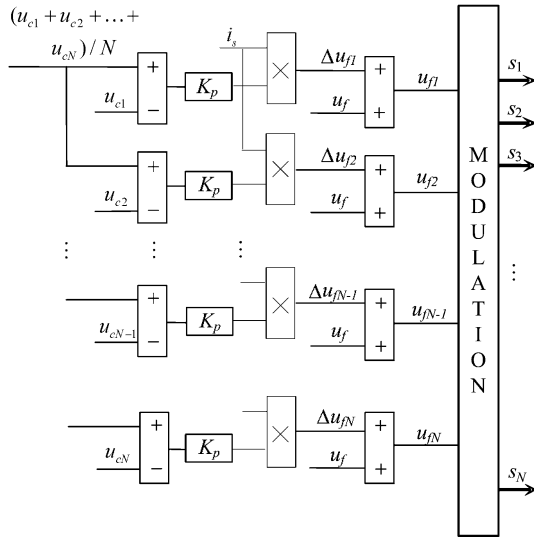


Fig. 7. Diagram of balance control strategy based on active voltage superposition.

balance control strategy is shown in Fig. 9 by analogy, where $\dot{u}_{f1}, \dot{u}_{f2}, \dots, \dot{u}_{fN}$ are, respectively, the steady-state output voltage vector of chains after regulation through balance control strategy.

From Fig. 9, it yields

$$\sum_{n=1}^N \dot{u}_{fn} = \dot{u}_r. \quad (4)$$

Equation (4) shows that the balance control strategy based on active voltage vector superposition will not affect the upper layer control; the upper and lower layer controls are absolutely

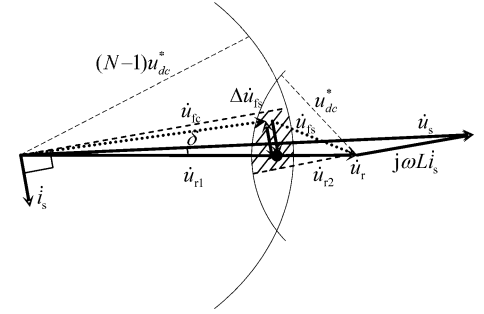


Fig. 8. Vector analysis of balance control strategy based on active voltage superposition.

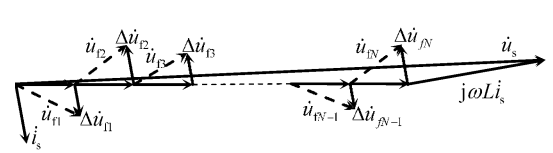


Fig. 9. Vector analysis of balance control strategy based on active voltage vector superposition for single link.

decoupled, the control strategy is with good stability and the controller parameters are simple to design.

B. Regulation Capacity Analysis of Balance Control Strategy

The regulation capacity refers to the maximum range of active power absorbed in chain through the balance control algorithm, it can be characterized by the active component of regulation voltage, also namely by the projection of regulation voltage at the direction of phase current. The regulation scope of balance

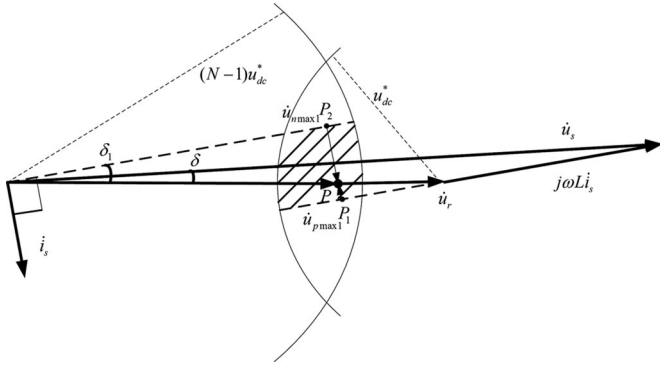


Fig. 10. Regulation range of balance control based on active voltage vector superposition.

control varies with different working conditions, but the possible maximum scope can be deduced under certain condition.

The maximum range based on active voltage vector superposition is shown in Fig. 10, P_1 and P_2 are the stable working points at maximum regulation range, \dot{u}_{pmax1} and \dot{u}_{nmax1} are, respectively, their projection in the current direction, where \dot{u}_{pmax1} denotes the maximum active voltage that can be increased and \dot{u}_{nmax1} denotes the maximum active voltage that can be reduced.

In Fig. 10, angle δ_1 can be got through modulation index M and phase-shift angle δ , which is obtained from decoupling control of upper layer

$$\delta_1 = \tan^{-1} \left(\frac{u_s \sin \delta}{u_s \cos \delta - NMu_{dc}^*} \right). \quad (5)$$

Then

$$u_{pmax1} = (N-1)Mu_{dc}^* \sin \delta_1 \quad (6)$$

$$u_{nmax1} = Mu_{dc}^* \sin \delta_1. \quad (7)$$

Assume that the active regulation range is $[-P_{h1} P_{h2}]$, then

$$P_{h1} = u_{pmax1} I_s = (N-1)Mu_{dc}^* \sin \delta_1 I_s \quad (8)$$

$$P_{h2} = u_{nmax1} I_s = Mu_{dc}^* \sin \delta_1 I_s. \quad (9)$$

IV. COMPARATIVE ANALYSIS OF BALANCE CONTROL STRATEGIES

Modulation index regulation and phase-shift angle regulation are two dc capacitor voltage balance control strategies commonly used in cascade multilevel STATCOM. A comparison is made among the proposed control strategy and this two. Their advantages and disadvantages are studied by the way of stability and regulation range analysis.

A. Control Diagram of Two Commonly Used Balance Strategy

1) *Strategy I: Control Diagram Based on Modulation Index Regulation:* The chain output voltage can be altered by modulation index regulation in the control strategy based on modulation index regulation. Its control diagram is shown in Fig. 11. The reference voltage is the average of homophase chains; the feedback is the actual of each chain, when the actual voltage is lower

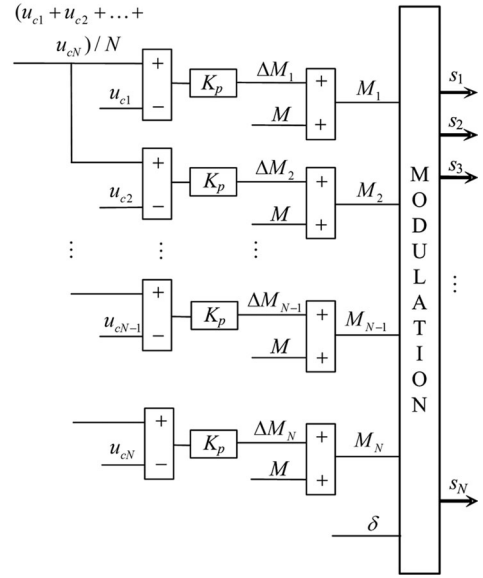


Fig. 11. Control diagram of balance control strategy based on modulation index regulation.

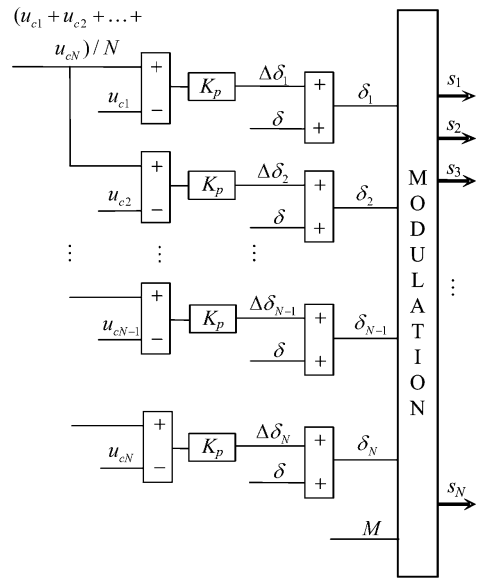


Fig. 12. Control diagram of balance control strategy based on phase-shift angle regulation.

than the reference. When the modulation index increases, the chain output voltage is also increased; when modulation index decreases, the chain output voltage also decreases.

2) *Strategy II: Control Diagram Based on Phase-Shift Angle Regulation:* The angle between chain output voltage and phase current can be altered by changing the phase-shift angle in the control strategy based on phase-shift angle regulation. Its control diagram is shown in Fig. 12.

In Fig. 12, the reference voltage is the average of homophase chains, the feedback is the actual of each chain; when the actual voltage is lower than the reference, the phase-shift angle is increased; otherwise the phase-shift angle is decreased.

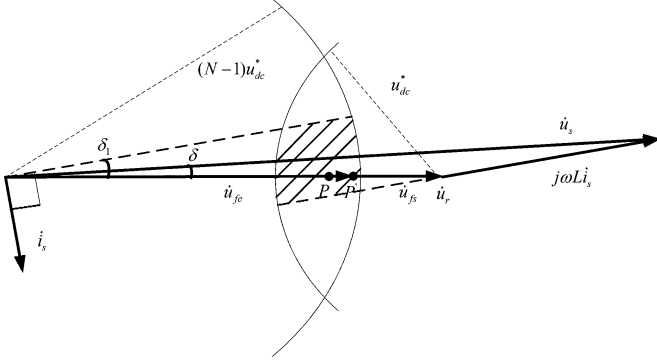


Fig. 13. Vector analysis of balance control strategy based on modulation index regulation.

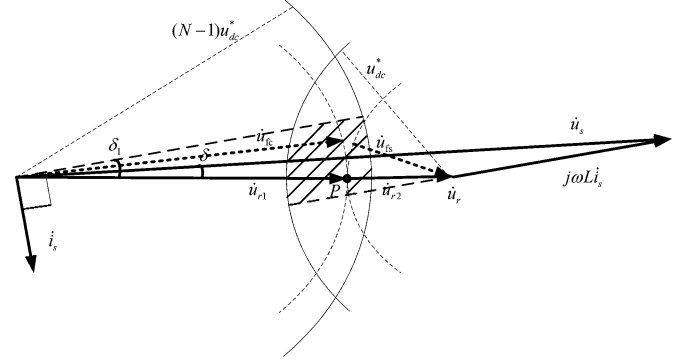


Fig. 15. Vector analysis of balance control strategy based on phase-shift angle regulation.

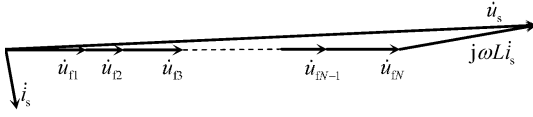


Fig. 14. Vector analysis of balance control strategy based on modulation index regulation for single link.

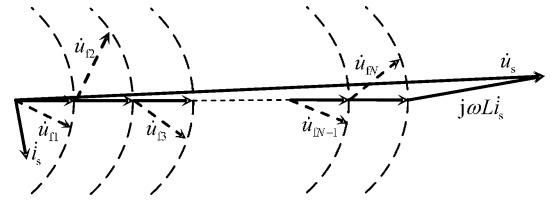


Fig. 16. Vector analysis of balance control strategy based on phase-shift angle regulation for single link.

B. Comparative Analysis of Stability for Balance Control Strategy

1) *Discussion I: Stability Analysis Based on Modulation Index Regulation:* The steady-state operating point moves in u_r only when modulation index is regulated, the vector diagram is shown in Fig. 13. The single-link vector diagram of balance control strategy is shown in Fig. 14 by analogy.

According to Fig. 14, the following equation can be obtained as

$$\sum_{n=1}^N \dot{u}_{fn} = \dot{u}_r. \quad (10)$$

Equation (10) shows that the balance control strategy based on modulation index regulation will not affect the upper layer control, the upper and lower layer controls are absolutely decoupled; the control strategy is with good stability and the controller parameters are simple to design.

2) *Discussion II: Stability Analysis Based on Modulation Index Regulation:* \dot{u}_{fc} moves in the circle with radius of $M(N-1)u_{dc}^*$, while vector \dot{u}_{fs} moves in the circle with radius of Mu_{dc}^* when only the phase-shift angle is regulated, and the vector diagram shown in Fig. 15, the two circles are tangent at point P ; therefore, there is no intersection point between \dot{u}_{fc} and \dot{u}_{fs} .

Then, the single-link vector diagram of balance control strategy is shown in Fig. 16, where $\dot{u}_{f1}, \dot{u}_{f2}, \dots, \dot{u}_{fN}$, respectively, move in the circle with radius of Mu_{dc}^* .

The conclusion can be obtained as the following:

$$\sum_{n=1}^N \dot{u}_{fn} \neq \dot{u}_r. \quad (11)$$

Equation (11) shows that the balance control strategy based on phase-shift angle regulation will affect the upper control; the

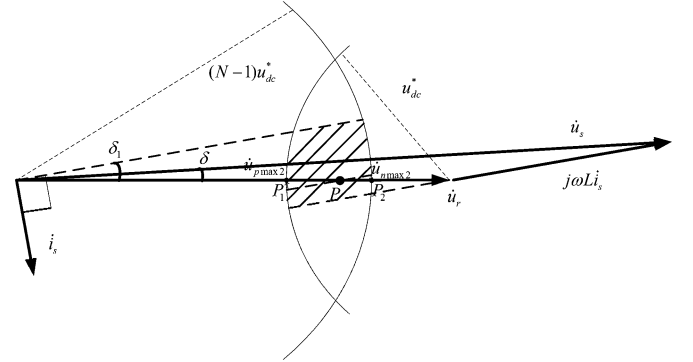


Fig. 17. Regulation range of balance control strategy based on modulation index regulation.

coupling exists between the upper and lower layer; therefore, the balance controller is difficult to design and improper designs will easily cause system instability.

C. Comparative Analysis of Regulations Capability for Balance Control Strategy

1) *Discussion I: Analysis of Regulations Capability Based on Modulation Index Regulation:* The maximum variation range of modulation index through the method of modulation index regulation is shown in Fig. 17, the active component of regulation voltage are, respectively, $\dot{u}_{p \max 2}$ and $\dot{u}_{n \max 2}$.

It can be derived as the following:

$$u_{p \max 2} = (1 - M)u_{dc}^* \sin \delta_1 \quad (12)$$

$$u_{n \max 2} = (N - 1)(1 - M)u_{dc}^* \sin \delta_1. \quad (13)$$

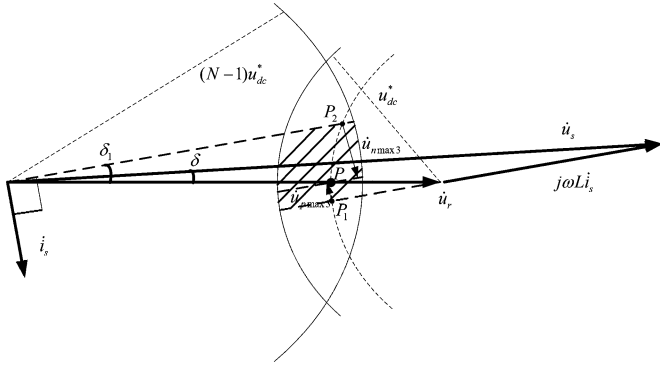


Fig. 18. Regulation range of balance control strategy based on phase-shift angle regulation.

Assuming that the active regulation range is $[-P_{M1} P_{M2}]$, then

$$P_{M1} = u_{p \max 2} I_s = (1 - M) u_{dc}^* \sin \delta_1 I_s \quad (14)$$

$$P_{M2} = u_{n \max 2} I_s = (N - 1)(1 - M) u_{dc}^* \sin \delta_1 I_s. \quad (15)$$

2) *Discussion II: Analysis of Regulations Capability Based on Modulation Index Regulation:* The maximum regulation range of phase-shift angle regulation is shown in Fig. 18, the active component of regulation voltage are, respectively, $\dot{u}_{p \max 3}$ and $\dot{u}_{n \max 3}$.

It can be obtained that

$$u_{p \max 3} = (N - 1) M u_{dc}^* \sin \delta_1 \quad (16)$$

$$u_{n \max 3} = M u_{dc}^* \sin \delta_1. \quad (17)$$

Assuming that the active regulation range is $[-P_{\delta 1} P_{\delta 2}]$, then

$$P_{\delta 1} = u_{p \max 3} I_s = (N - 1) M u_{dc}^* \sin \delta_1 I_s. \quad (18)$$

$$P_{\delta 2} = u_{n \max 3} I_s = M u_{dc}^* \sin \delta_1 I_s. \quad (19)$$

D. Comparative Analysis of Three Balance Control Strategies

1) *Conclusion I: Comparison of Stability:* From the comparative analysis of stability, it is known that for three kinds of balance control strategy:

- 1) the upper and lower layer controls in the balance control strategies based on active voltage vector superposition and modulation index regulation are absolutely decoupled and the parameters of balance controller are easy to design;
- 2) the upper layer and lower layer control in the balance control strategy based on phase-shift angle regulation are coupled with each other;
- 3) the balance control strategies based on active voltage vector superposition and modulation index regulation are of strong stability, and the balance control strategy based on phase-shift angle regulation is susceptible to interference.

2) *Conclusion II: Comparison of Regulation Range:* On comparing (8), (9), (14), (15), (18), and (19), it can be obtained

that when $(N - 1)/N \leq M \leq 1$

$$\begin{cases} P_{M1} < P_{h1} = P_{\delta 1} \\ P_{M2} < P_{h2} = P_{\delta 2} \end{cases} \quad (20)$$

Analyzing Fig. 3(b) by the same method, when $1/N \leq M \leq (N - 1)/N$

$$\begin{cases} P_{M1} = (1 - M) u_{dc}^* \sin \delta_1 I_s \\ P_{M2} = M u_{dc}^* \sin \delta_1 I_s \\ P_{\delta 1} = (N - 1) M u_{dc}^* \sin \delta_1 I_s \\ P_{\delta 2} = M u_{dc}^* \sin \delta_1 I_s \\ P_{h1} = (N - 1) M u_{dc}^* \sin \delta_1 I_s \\ P_{h2} = M u_{dc}^* \sin \delta_1 I_s \end{cases} \quad (21)$$

Then

$$\begin{cases} P_{M1} < P_{h1} = P_{\delta 1} \\ P_{M2} = P_{h2} = P_{\delta 2} \end{cases} \quad (22)$$

Similarly from Fig. 3(c), when $0 < M \leq 1/N$

$$\begin{cases} P_{M1} = (N - 1) M u_{dc}^* \sin \delta_1 I_s \\ P_{M2} = M u_{dc}^* \sin \delta_1 I_s \\ P_{\delta 1} = (N - 1) M u_{dc}^* \sin \delta_1 I_s \\ P_{\delta 2} = M u_{dc}^* \sin \delta_1 I_s \\ P_{h1} = (N - 1) M u_{dc}^* \sin \delta_1 I_s \\ P_{h2} = M u_{dc}^* \sin \delta_1 I_s \end{cases} \quad (23)$$

Therefore,

$$\begin{cases} P_{M1} = P_{h1} = P_{\delta 1} \\ P_{M2} = P_{h2} = P_{\delta 2} \end{cases} \quad (24)$$

Analyzing the regulation range of three types of balance control strategy, it can be concluded that:

- 1) the regulation range is related with the modulation index for three types of balance control strategy;
- 2) the regulation capability of balance control strategy based on active voltage vector superposition is the same as that of balance control strategy based on phase-shift angle regulation;
- 3) the regulation capability of balance control strategy based on modulation index regulation is the same as the other two when the modulation is small, but it is smaller than the others when the modulation is big.

Through the comparative analysis of stability and regulation range, it is known that the presented balance control strategy based on active voltage vector superposition is best.

V. SIMULATION VERIFICATION OF THREE TYPES OF BALANCE CONTROL STRATEGY

A. Parameters of Simulation System

The three types of control strategy are verified by simulation, the system parameters are shown in Table I.

To verify the balance control strategies, take the dc-side shunt resistor of one chain to be R and that of all other chains are $1 \text{ k}\Omega$, which can cause difference of shunt loss among chains.

When cascade multilevel works in inductive mode and absorbs rated reactive current, the modulation index is as follows:

$$M = (u_s - I_{\text{ref}} \omega L) \times \sqrt{2}/N/u_{dc} = 0.61.$$

TABLE I
SPECIFICATIONS OF SIMULATION

Parameters	Values
Three-phase line voltage u_s/V	6000
System frequency f_s/Hz	50
Output inductor L_s/mH	28.6
DC-side capacitor $C_{dc}/\mu F$	1840
DC-side capacitor voltage u_{dc}/V	1000
Carrier phase-shifting with single polarity double frequency f_c/Hz	250
Chain number N	12
Output reactive current reference I_{ref}/A	100

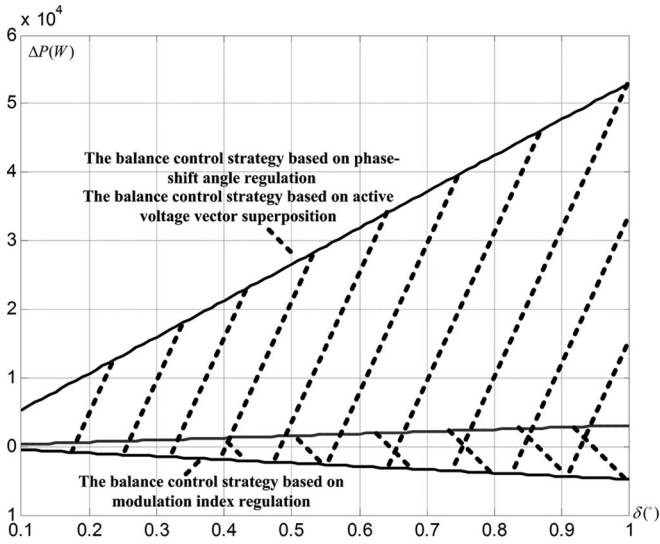


Fig. 19. Contrast of regulation range.

Figure out the regulation range of three types of balance control strategy according to modulation index, which is shown in Fig. 19, where $M = 0.61$, $\delta \in [0.1^\circ 1^\circ]$.

When $R = 500 \Omega$, the shunt loss difference among chains is as follows:

$$\Delta P = \frac{u_{dc}^2}{500} - \frac{u_{dc}^2}{1000} = 1 \text{ kW.}$$

When $R = 200 \Omega$, the shunt loss difference among chains is as follows:

$$\Delta P = \frac{u_{dc}^2}{200} - \frac{u_{dc}^2}{1000} = 4 \text{ kW.}$$

B. Simulation Without Balance Control Strategy

The dc-side capacitor voltage waveforms are shown in Fig. 20, when shunt loss difference among chains exists and no balance control strategy is adopted. Fig. 20 shows that the shunt loss difference will cause serious imbalance of capacitor voltage for cascade multilevel STATCOM. When $R = 200 \Omega$, the maximum difference of dc capacitor voltage among chains is 973 V, and

when $R = 500 \Omega$, the maximum difference of dc capacitor voltage among chains is 578 V.

C. Simulation of Balance Control Strategy Based on Modulation Index Regulation

Fig. 19 shows that the dc capacitor voltage of cascade multilevel STATCOM can be maintained balanced when shunt resistance is 500Ω , but it exceeds its balance regulation range when shunt resistance is 200Ω . The conclusions are verified by simulation, the simulation waveforms of $R = 500 \Omega$ are shown in Fig. 21, while that of $R = 200 \Omega$ are shown in Fig. 22.

Fig. 21 shows that the dc capacitor voltage of cascade multilevel STATCOM can be balanced through the control strategy of modulation index regulation, there is a certain steady-state error for proportional control, and the maximum difference of capacitor voltage is 20 V.

Fig. 22(a) shows that the maximum difference is 220 V when the proportion coefficient $K_p = 15$; therefore, the capacitor voltage difference can be reduced by the control strategy of changing modulation index, but it still exists a large steady-state error. Fig. 22(b) shows that the system oscillation has occurred when the proportion coefficient K_p is increased to 16, which indicates that the capacitor voltage cannot be balanced by the control strategy of changing modulation index under this condition.

D. Simulation of Balance Control Strategy Based on Phase-Shift Angle Regulation

The dc-side capacitor voltage waveform through the balance control strategy based on phase-shift angle regulation is shown in Fig. 23, when the shunt resistance $R = 200 \Omega$. The maximum difference of capacitor voltage is 15 V; therefore, the capacitor voltage can be balanced by the control strategy of phase-shift angle regulation even if the shunt loss is quite different, but the proportional coefficient K_p cannot exceed 13; therefore, the adjustment range is rather small.

E. Simulation of Balance Control Strategy Based on Active Voltage Vector Superposition

The dc-side capacitor voltage waveform through the balance control strategy based on active voltage vector superposition is shown in Fig. 24, when the shunt resistance $R = 200 \Omega$. It can be seen that the maximum difference of capacitor voltage is 14 V; therefore, the balance of dc capacitor voltage is achieved perfectly. Meanwhile, the value of K_p can be ranged to 950; therefore, adjustment range is rather wide.

VI. EXPERIMENTAL RESULTS

A. Description of Experimental System

A prototype of cascade multilevel STATCOM has been developed to verify the proposed control strategy and compensation modes, the structure of this prototype is still the same as that shown in Fig. 1 with delta connection and 12 chains in each phase. The parameters of prototype are shown in Table II.

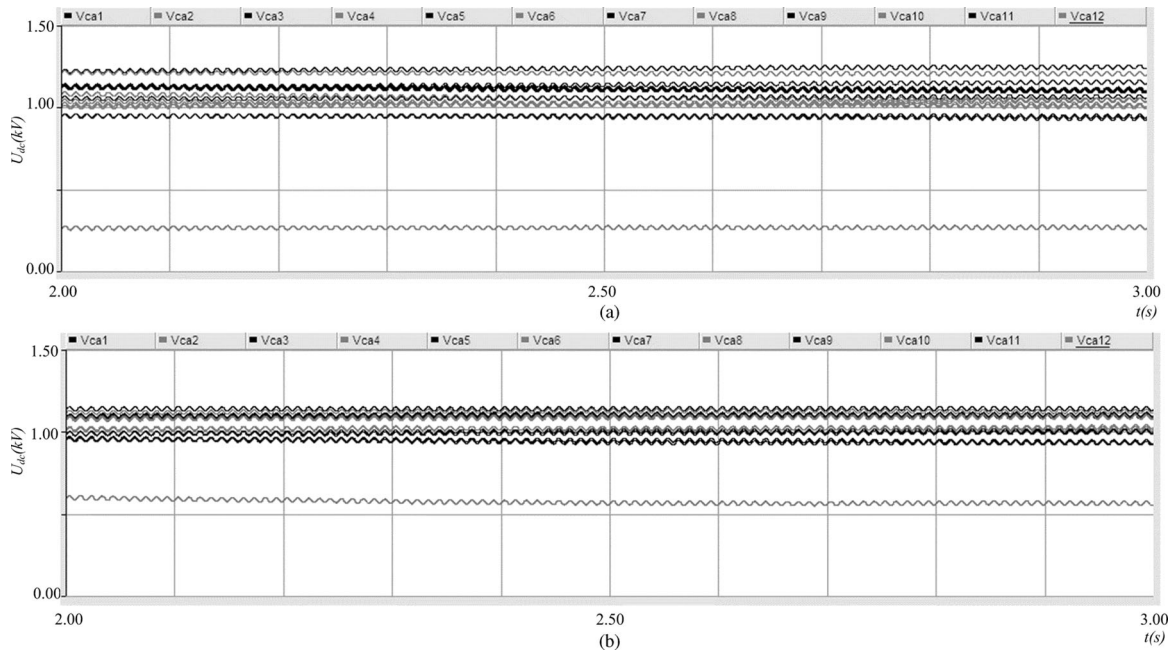


Fig. 20. DC capacitor voltage waveforms without balance control strategy. (a) $R = 200 \Omega$. (b) $R = 500 \Omega$.

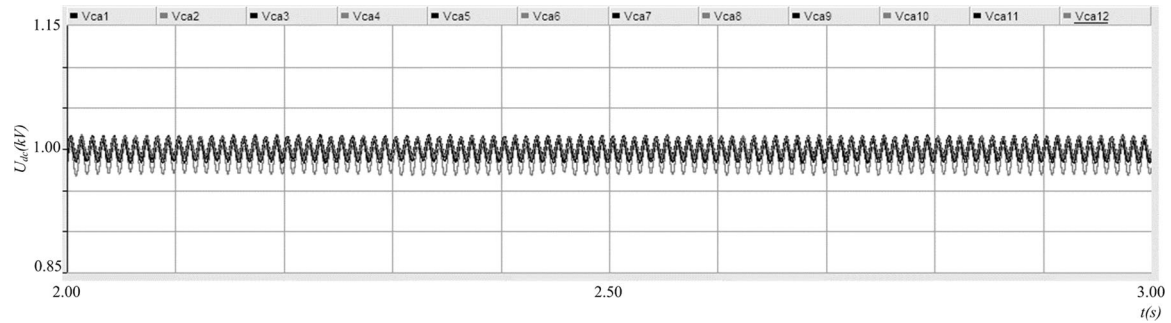


Fig. 21. DC capacitor voltage waveforms of $R = 500 \Omega$ through the control strategy of modulation index regulation.

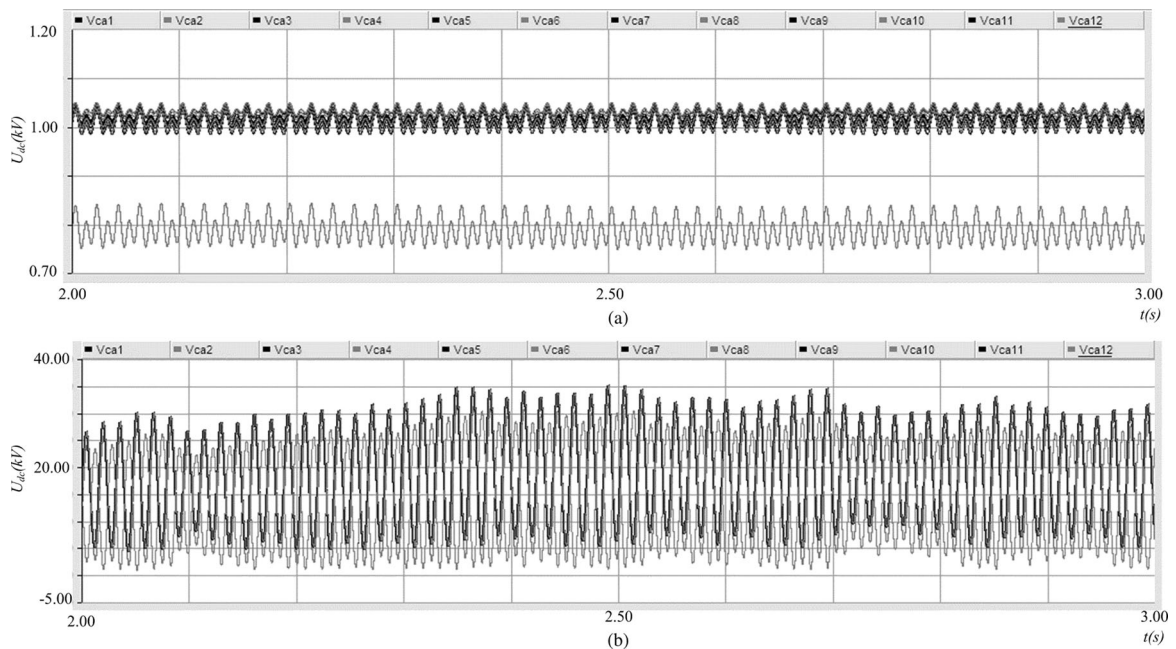


Fig. 22. DC capacitor voltage waveforms of $R = 200 \Omega$ through the control strategy of modulation index regulation. (a) $R = 200 \Omega$ and $K_p = 15$. (b) $R = 200 \Omega$ and $K_p = 16$.

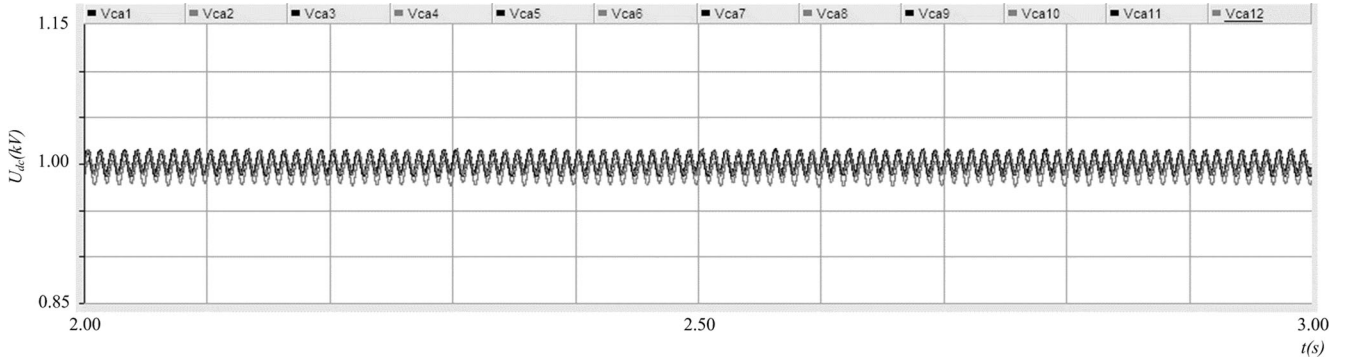


Fig. 23. DC capacitor voltage waveforms of $R = 200 \Omega$ through the control strategy of phase-shift angle regulation.

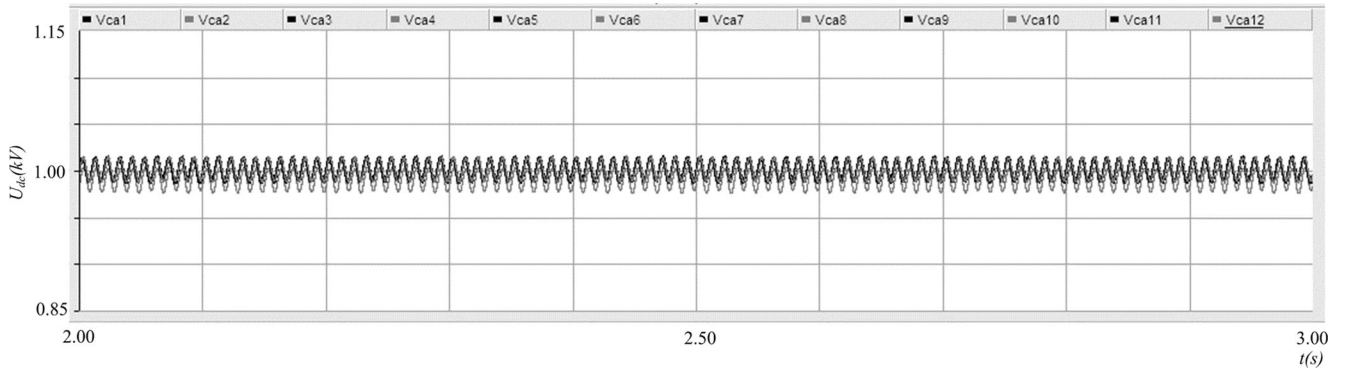


Fig. 24. DC capacitor voltage waveforms of $R = 200 \Omega$ through the control strategy of active voltage superposition.

TABLE II
SPECIFICATIONS OF PROTOTYPE

Parameter	Value	Description
u_s/V	380	Three-phase line voltage
f_s/Hz	50	System frequency
L_s/mH	5	Joint inductance
$C_{dc}/\mu F$	940	DC-side capacitor
u_{dc}/V	50	DC-side capacitor voltage
i_{ref}/A	2.5	Reactive current reference
f_c/Hz	250	Carrier phase-shifting with single polarity double frequency
N	12	Chain numbers

Fig. 25 shows the main circuit and controller of prototype, a concurrent hardware based on an association between DSP TM320F28335 and dual field programmable gate array (FPGA) XC3S250 was constructed to realize the control scheme shown in Fig. 2. The DSP is dedicated to realize the current control loop; one FPGA is dedicated to generate the PWM gating signals and the other is dedicated to achieve communications and protections.

The shunt resistance of one chain is set as $50 \text{ k}\Omega$, while the others are set to be $100 \text{ k}\Omega$; therefore, their shunt losses

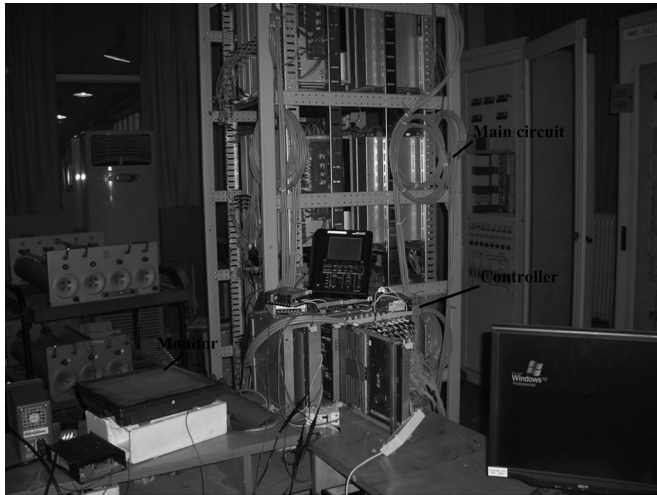
are different. A comparison is made on dc capacitor voltage distribution among link AB between situations with and without balance control, and the controller parameters are obtained through experiment and simulation.

B. Experimental Verification of Balance Control Strategy

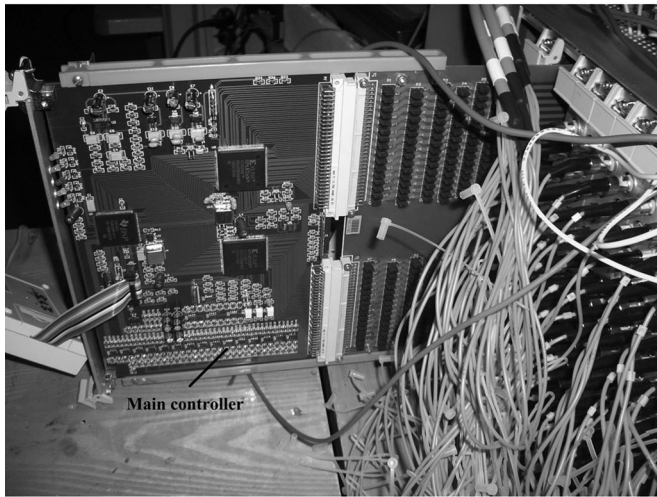
The capacitor voltage distributions with and without balance control are listed in Table III from the industrial personal computer (IPC).

Fig. 26(a) shows the waveforms of system voltage, link output voltage, and phase current of phase AB without balance control strategy; Fig. 26(b) is the THD of link output voltage. It is known that the capacitor voltage is very inconsistent without balance control; the maximum voltage is 65 V , while the minimum voltage is 34 V ; the maximum difference is 31 V and the THD of output voltage is 2.613% .

Fig. 27(a) shows the waveforms of system voltage, link output voltage, and phase current of phase AB with balance control strategy; Fig. 27(b) is the THD of link output voltage. It can be known that the capacitor voltage tends to be identical with balance control; the maximum voltage is 54 V , while the minimum voltage is 52 V ; the maximum difference is 2 V and the THD of output voltage is reduced to 2.496% . Comparing Fig. 26 with Fig. 27, the effectiveness and feasibility of proposed balance algorithm are proved.



(a)

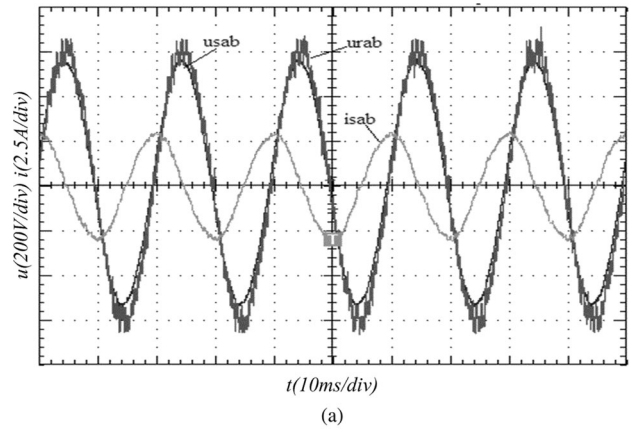


(b)

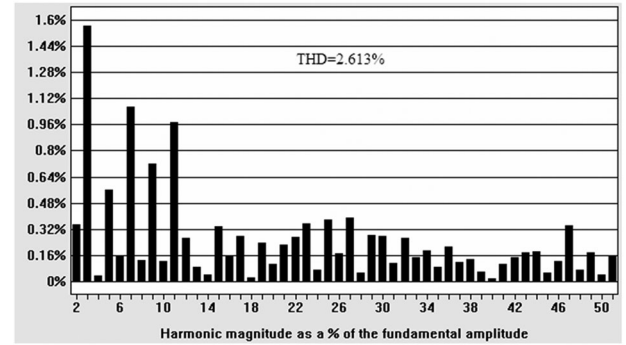
Fig. 25. Prototype of cascade multilevel STATCOM. (a) Main circuit. (b) Main controller.

TABLE III
CAPACITOR VOLTAGE DISTRIBUTIONS WITH AND WITHOUT BALANCE CONTROL

Chain numbering	Without balance control (V)	With balance control (V)
1	65	53
2	53	52
3	52	53
4	60	53
5	43	53
6	57	54
7	62	53
8	52	53
9	59	53
10	51	52
11	62	53
12	34	54

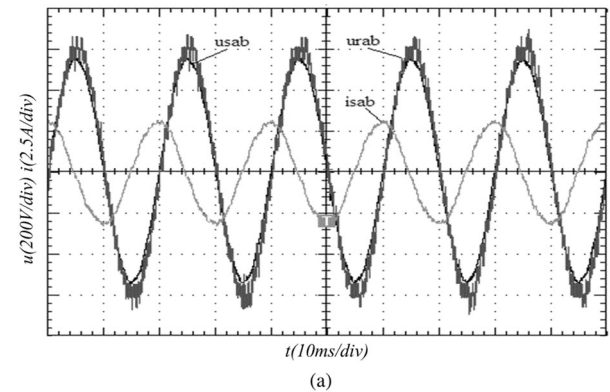


(a)

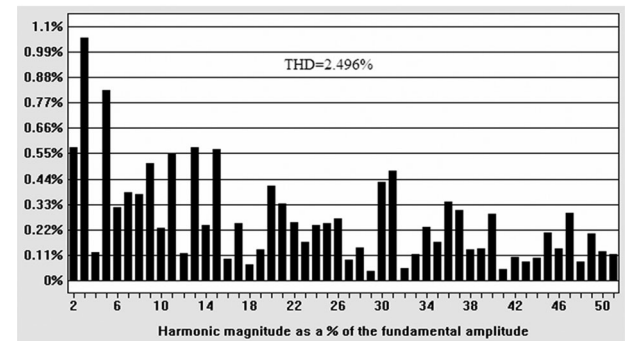


(b)

Fig. 26. Experiment of phase AB without balance control. (a) Waveforms of system voltage, link output voltage, and phase current. (b) THD of link output voltage.



(a)



(b)

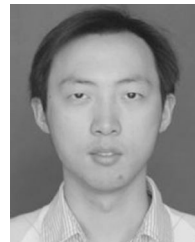
Fig. 27. Experiment of phase AB with balance control. (a) Waveforms of system voltage, link output voltage, and phase current. (b) THD of link output voltage.

VII. CONCLUSION

This paper has proposed a novelty dc capacitor voltage balance control strategy for cascade multilevel STATCOM. The dc capacitor voltage imbalance is caused by the difference of absorbed power and power loss among chains; hence, the dc capacitor voltage balance can be achieved through changing the absorbed power of chain, on this basis three types of balance control strategy are discussed and one of them is presented based on active voltage vector superposition. The control diagram of proposed method is illustrated, in addition, stability and regulation range are analyzed through vector analysis. Comparing the proposed method with the other two commonly used balance control strategies by vector analysis, the proposed method has the following advantages: 1) it is absolutely decoupled with the upper layer control; therefore, it has good control performance and the control parameters are easy to design and 2) its regulation capability is rather strong. In this paper, all the theoretical analysis is verified by simulation and also a prototype of cascade multilevel STATCOM is developed to prove it. Simulation and experimental results show that the problem of dc capacitor voltage balance for cascade multilevel can be effectively solved by the balance control strategy of active voltage vector superposition.

REFERENCES

- [1] D. Soto and T. C. Green, "A comparison of high-power converter topologies for the implementation of FACTS controllers," *IEEE Trans. Ind. Electron.*, vol. 49, no. 5, pp. 1072–1080, Oct. 2002.
- [2] C. K. Lee, J. S. K. Leung, S. Y. R. Hui, and H. S.-H. Chung, "Circuit-level comparison of STATCOM technologies," *IEEE Trans. Power Electron.*, vol. 18, no. 4, pp. 1084–1092, Jul. 2003.
- [3] T. An, M. T. Powell, H. L. Thanawala, and N. Jenkins, "Assessment of two different STATCOM configurations for FACTS application in power systems," presented at the Int. Conf. Power Syst. Technol., Beijing, China, 1998.
- [4] J. D. Ainsworth, M. Davies, P. J. Fitz, K. E. Owen, and D. R. Trainer, "Static var compensator (STATCOM) based on single-phase chain-circuit converters," *Proc. IEE—Gen., Transm., Distrib.*, vol. 145, no. 4, pp. 381–386, Jul. 1998.
- [5] S. Sirisukprasert, "The modeling and control of a cascaded-multilevel converter-based STATCOM," Ph.D. dissertation, Dept. Electr. Eng., Va. Polytechnic Inst. State Univ., Blacksburg, VA, Feb. 2004.
- [6] F. Z. Peng, W. S. John, and D. A. Adams, "A power line conditioner using cascade multilevel inverters for distribution systems," *IEEE Trans. Ind. Appl.*, vol. 34, no. 6, pp. 1293–1298, Nov./Dec. 1998.
- [7] Q. Song, W. Liu, and Z. Yuan, "Multilevel optimal modulation and dynamic control strategies for STATCOMs using cascaded multilevel inverters," *IEEE Trans. Power Del.*, vol. 22, no. 3, pp. 1937–1946, Jul. 2007.
- [8] M. S. A. Dahidah and V. G. Agelidis, "Selective harmonic elimination PWM control for cascaded multilevel voltage source converters: A generalized formula," *IEEE Trans. Power Electron.*, vol. 23, no. 4, pp. 1620–1630, Jul. 2008.
- [9] D. J. Hanson, M. L. Woodhouse, C. Horwill, D. R. Monkhouse, and M. M. Osborne, "STATCOM: A new era of reactive compensation," *Power Eng. J.*, vol. 16, no. 3, pp. 151–160, 2002.
- [10] M. L. Woodhouse, M. W. Donoghue, and M. M. Osborn, "Type testing of the GTO valves for a novel STATCOM converter," presented at the 7th Int. Conf. AC–DC Power Transm., London, U.K., 2001.
- [11] W. Jun and K. M. Smedley, "Synthesis of multilevel converters based on single- and/or three-phase converter building blocks," *IEEE Trans. Power Electron.*, vol. 23, no. 3, pp. 1247–1256, May 2008.
- [12] C. H. Ng, M. A. Parker, R. Li, P. J. Tavner, J. R. Bumby, and E. Spooner, "A multilevel modular converter for a large, light weight wind turbine generator," *IEEE Trans. Power Electron.*, vol. 23, no. 3, pp. 1062–1074, May 2008.
- [13] J. Geng, "Modeling and controlling of cascade static synchronous compensator," Ph.D. dissertation, Dept. Electr. Eng., Tsinghua Univ., Beijing, China, 2003.
- [14] R. Naderi and A. Rahmati, "Phase-shifted carrier PWM technique for general cascaded inverters," *IEEE Trans. Power Electron.*, vol. 23, no. 3, pp. 1257–1269, May 2008.
- [15] Q. Song, W. Liu, Z. Yuan, W. Wei, and Y. Chen, "DC voltage balancing technique using multi-pulse optimal PWM for cascade H-bridge inverters based STATCOM," presented at the Appl. Power Electron. Conf. Expo., Anaheim, CA, 2004.
- [16] Y. Liang and C. O. Nwankpa, "A new type of STATCOM based on cascading voltage-source inverters with phase-shifted unipolar SPWM," *IEEE Trans. Ind. Appl.*, vol. 35, no. 5, pp. 1118–1123, Sep./Oct. 1999.
- [17] Y. Li and B. Wu, "A novel DC voltage detection technique in the CHB inverter-based STATCOM," *IEEE Trans. Power Del.*, vol. 23, no. 3, pp. 1613–1619, Jul. 2008.
- [18] J. A. Barrena, L. Marroyo, M. A. R. Vidal, and J. R. T. Apraiz, "Individual voltage balancing strategy for PWM cascaded H-Bridge converter based STATCOM," *IEEE Trans. Ind. Electron.*, vol. 55, no. 1, pp. 21–29, Jan. 2008.
- [19] J. A. Barrena, L. Marroyo, M. A. Rodriguez, O. Alonso, and J. R. Torrealday, "DC voltage balancing for PWM cascaded H-bridge converter based STATCOM," presented at the 32nd Annu. Conf. Ind. Electron., Paris, France, 2006.
- [20] H. Akagi, S. Inoue, and T. Yoshii, "Control and performance of a transformerless cascade PWM STATCOM with star configuration," *IEEE Trans. Ind. Appl.*, vol. 43, no. 4, pp. 1041–1049, Jul./Aug. 2007.
- [21] T. Yoshii, S. Inoue, and H. Akagi, "Control and performance of a medium-voltage transformerless cascade PWM STATCOM with star-configuration," presented at the Ind. Appl. Conf., Tampa, FL, 2006.
- [22] M. Hagiwara and H. Akagi, "Control and experiment of pulsewidth-modulated modular multilevel converters," *IEEE Trans. Power Electron.*, vol. 24, no. 7, pp. 1737–1746, Jul. 2009.
- [23] C. Han, Z. Yang, B. Chen, A. Q. Huang, B. Zhang, M. R. Ingram, and A.-A. Edris, "Evaluation of cascade-multilevel-converter-based STATCOM for arc furnace mitigation," *IEEE Trans. Ind. Appl.*, vol. 43, no. 2, pp. 378–385, Mar./Apr. 2007.
- [24] C. Ying, Q. Chang, M. L. Crow, S. Pekarek, and S. Atcitty, "A comparison of diode-clamped and cascaded multilevel converter for a STATCOM with energy storage," *IEEE Trans. Ind. Electron.*, vol. 53, no. 5, pp. 1512–1521, Oct. 2006.
- [25] L. Yu, S. Bhattacharya, S. Wenchao, and A. Q. Huang, "Control strategy for cascade multilevel inverter based STATCOM with optimal combination modulation," presented at the Power Electron. Spec. Conf., Rhodes, Greece, 2008.



Zhao Liu was born in Hubei Province, China, on June 28, 1983. He received the B.E. degree in electrical and electronic engineering from Huazhong University of Science and Technology, Wuhan, China, in 2006, where he is currently working toward the Ph.D. degree.

His current research interests include the application of power electronics in power system.



Bangyin Liu (M'10) received the B.S., M.S., and Ph.D. degrees in electrical engineering from Huazhong University of Science and Technology, Wuhan, China, in 2001, 2004, and 2008, respectively.

He is currently a Postdoctoral Research Fellow in the College of Electrical and Electronics Engineering, Huazhong University of Science and Technology. His research interests include renewable energy applications, soft-switching converters, and power electronics applied to power system.



Shanxu Duan received the B.E., M.E., and Ph.D. degrees in electrical engineering from Huazhong University of Science and Technology, Wuhan, China, in 1991, 1994, and 1999, respectively.

Since 1991, he has been a Faculty Member in the College of Electrical and Electronics Engineering, Huazhong University of Science and Technology, where he is currently a Professor. His research interests include stabilization, nonlinear control with application to power electronic circuits and systems, fully digitalized control techniques for power electronics apparatus and systems, and optimal control theory and corresponding application techniques for high-frequency pulsewidth-modulation power converters.

Dr. Duan is a Senior Member of the Chinese Society of Electrical Engineering and a Council Member of the Chinese Power Electronics Society. He was chosen as one of the New Century Excellent Talents by the Ministry of Education of China, in 2007, and was the recipient of the honor of "Delta Scholar" in 2009.



Yong Kang was born in Hubei Province, China, on October 16, 1965. He received the B.E. M.E, and Ph.D. degrees from Huazhong University of Science and Technology, Wuhan China, in 1988, 1991 and 1994, respectively.

He is currently the Head of the College of Electrical and Electronic Engineering, Huazhong University of Science and Technology, where he was a Lecturer in 1994, an Associate Professor in 1996, and Full Professor in 1998. He is the author of more than 60 technical papers. His research interests include power electronic converter, ac drivers, electromagnetic compatibility, and their digital control techniques.